HHS Public Access

Author manuscript

Mol Immunol. Author manuscript; available in PMC 2016 October 01.

Published in final edited form as:

Mol Immunol. 2015 October ; 67(2 0 0): 294–302. doi:10.1016/j.molimm.2015.06.013.

ATP binding by NLRP7 is required for inflammasome activation in response to bacterial lipopeptides

Alexander D. Radian[a,b], **Sonal Khare**[a], **Lan H. Chu**[a,b], **Andrea Dorfleutner**[a,*], and **Christian Stehlik**[a,c,*]

[a]Division of Rheumatology, Department of Medicine, Feinberg School of Medicine, Northwestern University, Chicago, IL 60611, USA

[b]Driskill Graduate Program in Life Sciences (DGP), Feinberg School of Medicine, Northwestern University, Chicago, IL 60611, USA

[c]Robert H. Lurie Comprehensive Cancer Center, Interdepartmental Immunobiology Center and Skin Disease Research Center, Feinberg School of Medicine, Northwestern University, Chicago, IL 60611, USA

Abstract

Nucleotide-binding oligimerization domain (NOD)-like receptors (NLRs) are pattern recognition receptors (PRRs) involved in innate immune responses. NLRs encode a central nucleotide-binding domain (NBD) consisting of the NAIP, CIITA, HET-E and TP1 (NACHT) domain and the NACHT associated domain (NAD), which facilitates receptor oligomerization and downstream inflammasome signaling. The NBD contains highly conserved regions, known as Walker motifs, that are required for nucleotide binding and hydrolysis. The NLR containing a PYRIN domain (PYD) 7 (NLRP7) has been recently shown to assemble an ASC and caspase-1-containing high molecular weight inflammasome complex in response to microbial acylated lipopeptides and *Staphylococcus aureus* infection. However, the molecular mechanism responsible for NLRP7 inflammasome activation is still elusive. Here we demonstrate that the NBD of NLRP7 is an ATP binding domain and has ATPase activity. We further show that an intact nucleotide-binding Walker A motif is required for NBD-mediated nucleotide binding and hydrolysis, oligomerization, and NLRP7 inflammasome formation and activity. Accordingly, THP-1 cells expressing a mutated Walker A motif display defective NLRP7 inflammasome activation, interleukin (IL)-1β release and pyroptosis in response to acylated lipopeptides and *S. aureus* infection. Taken together, our results provide novel insights into the mechanism of NLRP7 inflammasome assembly.

[*]Corresponding authors at: Division of Rheumatology, Department of Medicine, Feinberg School of Medicine, Northwestern University, Chicago, IL 60611, USA. Tel.: +1 312 503 3141; fax: +1 312 503 0994. a-dorfleutner@northwestern.edu (A. Dorfleutner), c-stehlik@northwestern.edu (C. Stehlik).

Authorship

A.D.R., S.K., L.H.C. and A.D. carried out the experiments. A.D. and C.S. designed the experiments. A.D.R., A.D. and C.S. wrote the manuscript and all authors reviewed and approved the final version.

Disclosures

None of the authors have any conflict of interest.

Keywords

Inflammation; IL-1β; Caspase-1; Nod like receptor; ATPase; *Staphylococcus aureus*

1. Introduction

The intracellular nucleotide-binding oligomerization domain (NOD)-like receptor (NLR) gene superfamily represents evolutionary-conserved innate immune pattern recognition receptors (PRRs). They detect pathogen-associated and damage-associated molecular patterns (PAMPs and DAMPs, respectively), and have been determined to trigger diverse pro-inflammatory host defense signaling pathways that contribute to pathogen clearance and wound healing, including inflammasome activation, activation of NF-κB and MAPK, and transcriptional control of MHC and related genes. NLRs are composed of a characteristic tripartite domain architecture featuring C-terminal ligand sensing and auto-regulatory leucine-rich repeats (LRRs), a central nucleotide-binding domain (NBD) comprised of the NACHT (NAIP, CIITA, HET-E and TP1) domain and NACHT-associated domain (NAD), and a variable N-terminal effector domain responsible for homo-typic protein–protein interactions, which enable downstream signaling. The 22 human members are sub-classified according to their effector domain as NLRA (containing an activation domain, AD), NLRB (containing a baculovirus inhibitor of apoptosis domain, BIR), NLRCs (containing a caspase activation and recruitment domain, CARD), NLRX (containing an X domain) and NLRPs (containing a PYRIN domain, PYD).

Several NLRs assemble inflammasomes, which are large, multi-protein signaling complexes consisting of NLRs, the adaptor protein apoptosis-associated speck-like protein containing a CARD (ASC) and caspase-1 (Martinon et al., 2002; Ratsimandresey et al., 2013; Schroder and Tschopp, 2010; Khare et al., 2010). Infection and tissue damage, as well as pathogen-, environmental- or host-derived danger signals trigger inflammasome formation, which subsequently leads to caspase-1 activation. Active caspase-1 is required for the proteolytic maturation and release of the pro-inflammatory cytokines interleukin (IL)-1β and IL-18 (Kostura et al., 1989; Thornberry et al., 1992; Fantuzzi et al., 1999; Ghayur et al., 1997; Kuida et al., 1995; Li et al., 1995), induction of pyroptosis (Fink and Cookson, 2006) and the release of alarmins and danger signals, including IL-1α, HMGB1 and inflammasome particles (Baroja-Mazo et al., 2014; Franklin et al., 2014; Groß et al., 2012; Lamkanfi et al., 2010; Willingham et al., 2009). The mechanism for inflammasome assembly involves ASC nucleation and the subsequent self-perpetuating polymerization of ASC (Cai et al., 2014; Lu et al., 2014; Man et al., 2014; Chu et al., 2015). Consequently polymerized ASC nucleates caspase-1 polymerization, which results in its activation (Stehlik et al., 2003a,b; Srinivasula et al., 2002). ASC nucleation is facilitated by NLRs and their ASC nucleation efficiency is enhanced upon NBD-dependent NLR oligomerization (Lu et al., 2014). NLRs belong to the signal transduction adenosine triphosphatases (ATPases) with numerous domains (STAND) subfamily within the ATPases associated with various cellular activities (AAA+) superfamily (Leipe et al., 2004; MacDonald et al., 2013). Since the 3D structure of a prototypical NACHT-NAD domain has not been resolved yet, it has only been characterized *in silico* by multiple sequence homology alignments, secondary structure prediction analyses

as well as homology modeling (MacDonald et al., 2013; Proell et al., 2008). The overall secondary structure is conserved between the NACHT-NAD domain and the NB-ARC domain of the apoptotic ATPase apoptotic peptidase activating factor 1 (APAF-1), another STAND family member (Reubold et al., 2011; Riedl et al., 2005). The NACHT domain consists of two distinct conserved regions. (1) The Walker A motif [GxxxxGK(S/T)], which forms the integral phosphate-binding loop (P-loop) and coordinates the β and γ phosphates of the nucleotide during hydrolysis (Eibl et al., 2012; MacDonald et al., 2013). Particularly, the highly conserved lysine residue is responsible for the coordination of the γ-phosphate (Traut, 1994). (2) The Walker B motif [(R/K)xxxxGxxxxLhhhhD], which is situated downstream of the Walker A motif in most P-loop proteins, is involved in the coordination of Mg^{2+} ions and contributes to ATP binding and ATPase catalytic activity (Iyer et al., 2004). The NAD is a C-terminal extension of the NACHT domain and shares significant homology with domains of APAF1 and contains a particular proline residue that is proposed to interact with the adenine ring of bound ATP (MacDonald et al., 2013). STAND proteins function as molecular switches, with the “OFF” position corresponding to a monomeric, resting ADP-bound form and the “ON” position corresponding to an ATP-bound, oligomeric form, competent of downstream signaling through the effector domains. Experimentally this model has been confirmed for NLRC4, where the LRR sterically blocks the NBD and sequesters NLRC4 in a monomeric state (Danot et al., 2009; Hu et al., 2013). Binding of an inducer to the sensor domain promotes ADP/ATP exchange and induces a conformational change resulting in protein activation by removing intramolecular inhibitory interactions, and hence facilitating oligomerization (Danot et al., 2009; Hu et al., 2013). Evidence for this nucleotide-dependent oligomerization model has been observed in several NLRPs. NLRP1 binds ATP, GTP, CTP, TTP and UTP to form a caspase-1-activating complex *in vitro* (Faustin et al., 2007), NLRP12 requires ATP binding activity in order to elicit its anti-inflammatory role (Ye et al., 2008) and NLRP3 inflammasome activation also depends on ATP binding and ATPase activity (Duncan et al., 2007). If the Walker A motif is experimentally mutated, these NLRs lose their function and even hereditary gain-of-function mutations in NLRP3, which cause Cryopyrinopathies, depend on nucleotide binding and lose their activity as a consequence of mutation of the Walker A motif (Duncan et al., 2007). However, Walker A mutations in NLRP1B result in an over-active protein, suggesting that mechanistic differences exist within the NLR family NBDs (Faustin et al., 2007).

NLRP7 belongs to the NLRP subfamily and forms an ASC and caspase-1-containing inflammasome in human macrophages in response to microbial acylated lipopeptides (acLP) and bacterial infection with *Staphylococcus aureus* and *Listeria monocytogenes* (Khare et al., 2012; Radian et al., 2013). Accordingly, NLRP7 is present in high molecular weight complexes following *S. aureus* infection (Khare et al., 2012). It has also been reported to co-localize with the Golgi and microtubules and inhibit IL-1β (Messaed et al., 2011a,b; Kinoshita et al., 2005). NLRP7 contains a predicted NBD domain and has recently been shown to self-associate through its NAD domain (Singer et al., 2014). However, it is currently unknown, if the NLRP7 NBD has ATPase activity and if this is involved in inflammasome activation.

In this study, we demonstrate for the first time that the NBD of NLRP7 binds ATP and exhibits ATPase activity and that this activity is required for NLRP7 oligomerization. We further show that an intact Walker A motif is necessary for NLRP7 inflammasome activation by acLPs and *S. aureus*. Thus, our results provide novel insights into the activation mechanism of NLRP7 and contribute to a better understanding of NLR activation.

2. Materials and methods

2.1. Materials and cell culture

The human embryonic kidney (HEK) 293 cell line was obtained from ATCC and maintained in DMEM containing 10% FBS and 100 IU/ml penicillin, 1 mg/ml streptomycin. THP-1 cells were obtained from ATCC and maintained in RPMI 1640 media, supplemented with 10% FBS, 1 mM sodium pyruvate, 1 mM HEPES buffer, 100 IU/ml penicillin, 1 mg/ml streptomycin, 2 mM glutamine, and 0.05 mM 2-mercaptoethanol. Cells were routinely tested for Mycoplasma contamination by PCR and TLR2 activation assay (Invivogen). Recombinant lentivirus was produced in HEK293-lenti cells (Clontech) by Xfect-based transfection (Clontech) with pLEX expression plasmids encoding myc-NLRP7 or myc-NLRP7^{WA} and the packaging plasmids pMD.2G and psPAX2 (Addgene plasmids 12259 and 12260), followed by filtration (0.45 μm). THP-1 cells were stably transduced with lentiviral particles in the presence of polybrene (0.5 μg/ml) using magnetic beads (ExpressMag, Sigma) or spinoculation and selected with Puromycin (0.5 μg/ml) for 2 weeks. Expression of NLRP7 and NLRP7^{WA} was verified by immunoblot. Cells were lysed in Laemmli buffer and cleared samples were separated by SDS-PAGE, transferred to PVDF membranes and analyzed by immunoblotting with anti-myc antibodies (Santa Cruz Biotechnology) and HRP-conjugated secondary antibodies (GE Healthcare), ECL detection (Pierce), and image acquisition (Ultralum). Cells were treated with FSL-1 (0.1 mg/ml), Pam3CSK4 (2 mg/ml), or HKAL (2×10^5 cfu/ml).

2.2. Plasmids

pcDNA3-based expression constructs for ASC, NLRP3, pro-caspase-1, pro-IL-1β and NLRP7 were described earlier (Bryan et al., 2010; Dorfleutner et al., 2007a,b; Khare et al., 2012; Stehlik et al., 2003a,b). NLRP7^{GKT183,184,185AAA} (NLRP7^{WA}) was generated by site directed mutagenesis and NLRP7^{NBD} by PCR (5′-CCGAATTCCCTGAGCTGGGAGATGCAGAAG-3′, 5′-GGCTCGAGTCCCAATGAAAGCAAGACAGA-3′) and cloned into pcDNA3-myc, pcDNA3-HA, pLEX-Myc and pGS-21a (GenScript) plasmids. All expression constructs were sequence verified.

2.3. Quantification of IL-1β secretion by ELISA

Culture supernatants were analyzed for IL-1β secretion by ELISA (BD Biosciences) according to the manufacturer's instructions.

2.4. Bacterial infection and caspase-1 activation

12×10^6 THP-1 cells were infected with *S. aureus* (MOI = 5), spinoculated at 500 g for 10 min, and incubated for the indicated times. To detect active caspase-1 by immunoblot, cells

were collected by centrifugation and lysed in Laemmli buffer. Cleared supernatants were TCA precipitated and resuspended in Laemmli buffer by sonication and analyzed by SDS/PAGE and immunoblotting using anti-caspase-1 p20 (Imgenex), and anti-active caspase-1 p20 (Cell Signaling) antibodies. For quantification of pyroptosis, 1.5×10^5 THP-1 cells were plated in triplicates in white 96-well plates and infected with *S. aureus* as above. Propidium iodide (1 μg/ml) was added to each well, and the cells were spinoculated for 5 min at 500 × *g*, PI binding to DNA was quantified by kinetic fluorescence reading in a Synergy HT microplate reader (Bio-Tek) at 37 °C using 525 nm absorbance and 620 nm excitation filters.

2.5. Inflammasome reconstitution system

The inflammasome reconstitution assay has been described earlier (Bryan et al., 2010; Dorfleutner et al., 2007a,b; Khare et al., 2012; Stehlik et al., 2003a,b). Briefly, HEK293 cells were transfected in 12-well dishes with expression constructs for mouse pro-IL-1β, pro-caspase-1, ASC and NLRs using Xfect (Clontech). Where indicated, cells were transfected 24 h after the first transfection with transfection mixture or FSL-1 (500 ng) with Lipofectamine 2000. Culture supernatants were collected 12 h post-transfection, clarified by centrifugation and analyzed for IL-1β secretion by ELISA or caspase-1 activation was determined by immunoblot in total cell lysates. Expression of all cDNAs was verified by SDS/PAGE and immunoblot in total cell lysates.

2.6. Recombinant GST protein purification

BL21 *Escherichia coli* was transformed with pGS-21a bacterial expression plasmids encoding GST, GST-NLRP7^{NBD}, and GST-NLRP7$^{NBD(WA)}$. Cultures were grown overnight, diluted 1:20, and then grown until an OD_{600} of 0.5. Recombinant protein expression was induced using 0.4 mM IPTG for 6 h at 37 °C, followed by repetitive freeze-thaw lysis of bacteria in PBS. Lysates were adjusted to 1 mg/ml lysozyme, 1 mM PMSF, 1 mM DTT, 2% Sodium lauroyl sarcosinate, 4% Triton X-100, 10 mM CHAPS and GST proteins were affinity purified using Glutathione Resin (GenScript).

2.7. GST pull–down

HEK293N cells were plated in 6-well plates (2×10^6 cells/well) and transfected with expression constructs encoding either myc-NLRP7 or myc-NLRP7^{NBD}. 48 h post transfection, cells were lysed (50 mM Tris–HCl pH 7.5, 100 mM NaCl, 0.5% Triton X-100, 1 mM Sodium Pyrophosphate, 2 mM $MgCl_2$, 1 mM PMSF, supplemented with 1 × Protease Inhibitor Cocktail (Roche)) for 30 min on ice. Total cell lysates (TCL) were clarified by centrifugation, and incubated on a nutator at 4 °C for 4 h with glutathione resin-immobilized GST or GST-NLRP7^{NBD} (1 μg). Beads were washed 3× with lysis buffer and eluted in 30 μl 2× Laemmli buffer. Co-purified proteins were resolved by SDS/PAGE and immunoblot using rabbit anti-myc antibody (Santa Cruz Biotechnology) and HRP-conjugated secondary antibodies, ECL detection (Pierce), and image acquisition (Ultralum). TCL (5–10%) were also analyzed where indicated.

2.8. Co-immunoprecipitation

HEK293N cells were transfected as above with myc-NLRP7^{NBD}, myc-NLRP7$^{NBD(WA)}$, HA-NLRP7^{NBD}, or HA-NLRP7$^{NBD(WA)}$. 48 h post transfection, cells were lysed (50 mM Tris–HCl pH 7.5, 180 mM NaCl, 0.5% Triton X-100, 1 mM Sodium Pyrophosphate, 2 mM $MgCl_2$, 1 mM PMSF, 1 mM ATP, supplemented with 1× protease inhibitor cocktail (Roche)) for 30 min on ice. TCL were clarified by centrifugation, and incubated on a nutator at 4 °C for 4 h with agarose bead-immobilized mouse anti-myc antibody (Santa Cruz Biotechnology). Bound proteins were washed 3× in lysis buffer, eluted in 30 μl 2× Laemmli buffer and detected by SDS/PAGE immunoblotting using directly HRP-conjugated anti-HA and anti-myc antibodies (Santa Cruz Biotechnology).

2.9. ATP-binding assay

HEK293N cells were transfected as above, lysed (50 mM Tris–HCl pH 7.5, 100 mM NaCl, 0.5% Triton X-100, 1 mM Sodium Pyrophosphate, 2 mM $MgCl_2$, 1 mM PMSF, supplemented with 1× protease inhibitor cocktail (Roche)), clarified by centrifugation, where indicated, supplemented with ATP and incubated with 3% BSA blocked control agarose and agarose-immobilized ATP (Sigma) on a nutator at 4 °C for 4 h. Bound proteins were washed 3× with lysis buffer and eluted in 30 μl 2× Laemmli buffer and detected by SDS/PAGE immunoblotting using anti-myc antibodies (Santa Cruz Biotechnology).

2.10. ATPase assay

NLRP7 ATPase activity was determined using the ADP-Glo Kinase Assay (Promega), according to manufacturer's protocol. ADP-generating enzyme activity is detected after depletion of remaining ATP and conversion of the generated ADP to ATP, which is then measured using a luciferase/luciferin reaction. Luminescence is correlated to ADP concentrations by using an ATP-to-ADP conversion curve. Briefly, 25 μL reactions were performed in 96-well plates using 1 μg recombinant protein in enzyme buffer (50 μM ATP, 40 mM Tris–HCl pH 7.5, 20 mM $MgCl_2$, 0.1 mg/ml BSA) at 25 °C for 2 h. Luminescence was measured using a Synergy HT Microplate Reader (Bio-Tek).

2.11. Size exclusion chromatography

Size exclusion chromatography (SEC) was performed as previously described (Khare et al., 2012). HEK293N cells were transiently transfected as described above. 9×10^6 cells were lysed in SEC lysis buffer (20 mM Tris–HCl pH 7.4, 150 mM NaCl, 1% octylglucoside, 1 mM $MgCl_2$, 1 mM ATP, supplemented with 1× Roche protease inhibitor cocktail), followed by Dounce homogenization on ice. TCL was cleared by centrifugation (13,000 × *g* at 4 °C for 30 min) and then filtered (0.45 μM). TCL and MW standards were subjected to SEC on a 16 mm × 600 mm HiPrep Sephacryl S300HR column (GE Healthcare) in SEC running buffer (50 mM Tris pH 7.4, 150 mM NaCl) at 4 °C at a flow rate of 0.5 ml/min. Individual fractions were TCA precipitated, dissolved in Laemmli buffer and NLRP7 detected as described above.

2.12. Statistical analysis

Graphs were prepared in Prism 5 (GraphPad) and represent the mean ± s.e.m A standard two-tailed unpaired *t*-test was used for statistical analysis of two groups and 2 way ANOVA for kinetic analyses with all data points showing a normal distribution. Values of $P < 0.05$ were considered significant.

3. Results

3.1. NLRP7 contains a predicted nucleotide-binding domain (NBD) and is sufficient for dimerization

The NBD is responsible for nucleotide binding in NLRC1, NLRC2, NLRC4, NLRP1, NLRP3 and NLRP12 (Duncan et al., 2007; Faustin et al., 2007; Lu et al., 2005; Ye et al., 2008), or required for nuclear import and transactivation in NLRA (CIITA) and NLRC5 (Harton et al., 1999; Meissner et al., 2012). NLPR7 also harbors a central NBD domain ($NLRP7^{NBD}$) with considerable homology to other NLRs. The NBD can be divided into a NACHT and NAD, but the NACHT contains the conserved nucleotide binding motifs including the ATP-specific phosphate binding loop (Walker A motif) (Koonin and Aravind, 2000; Albrecht et al., 2003). CLUSTALW sequence alignment of the $NLRP7^{NBD}$ with the NBDs of NLRPs with experimentally demonstrated nucleotide binding and/or hydrolysis activities, namely NLRP3, NLRP1, and NLRP12, shows that NLRP7 contains the conserved Walker A motif (Fig. 1A and Supplemental Fig. 1). We have previously shown that NLRP7 is capable of forming high-order multimeric inflammasome complexes in primary human macrophages (Khare et al., 2012), but it is unclear if specifically the NBD contributes to NLRP7 self-oligomerization. To determine homomeric NBD binding, we purified the GST-tagged $NLRP7^{NBD}$ from bacteria and used it in GST pull-down assays. GST-$NLRP7^{NBD}$, but not GST control was able to pull-down Myc-tagged $NLRP7^{NBD}$ from transiently transfected HEK293 cells (Fig. 1B). We verified this finding in cells by co-immunoprecipitation following co-expression of Myc and HA-tagged $NLRP7^{NBD}$ (Fig. 1C), indicating that the NBD is sufficient for NLRP7 oligomerization.

Supplementary Fig. S1 related to this article can be found, in the online version, at http://dx.doi.org/10.1016/j.molimm.2015.06.013

3.2. The Walker A motif in the $NLRP7^{NBD}$ is required for oligomerization

Due to the presence of predicted Walker motifs involved in nucleotide binding and hydrolysis, we hypothesized that homomeric NLRP7 interactions will require this activity. We therefore mutated the predicted Walker A motif represented by G^{183}, K^{184}, and T^{185} in NLRP7 by site-directed mutagenesis to alanine, thus generating the $NLRP7^{WA}$ mutant (Fig. 2A). To test whether nucleotide binding is required for $NLRP7^{NBD}$ self-association, myc-tagged $NLRP7^{NBD}$ was co-transfected with HA-tagged $NLRP7^{NBD}$ or $NLRP7^{NBD(WA)}$ into HEK293 cells and myc-containing $NLRP7^{NBD}$ protein complexes were immunoprecipitated. In agreement with our *in vitro* pull down result, we observed that the $NLRP7^{NBD}$ was able to self-associate (Fig. 2B). Although $NLRP7^{NBD}$ was still able to associate with $NLRP7^{NBD(WA)}$, this interaction was substantially weakened (Fig. 2B). However, self-association of myc- and HA-tagged $NLRP7^{NBD(WA)}$ was almost completely

prevented (Fig. 2C). These findings suggest that NLRP7 requires an intact Walker A motif to mediate self association through its NBD. Although the PYD can undergo homotypic interactions, we hypothesized that nucleotide binding by NLRP7 would be required for high-order complex formation. To directly test this model, we used gel filtration chromatography to determine the formation of NLRP7 oligomers. Transfection of NLRP7 into HEK293 cells, which are deficient in endogenous NLRP7, is sufficient to cause NLRP7 inflammasome activation (Khare et al., 2012). We therefore transiently transfected either NLRP7 or NLRP7^{WA} into HEK293 cells and subjected cell lysates to size fractionation, and analyzed individual fractions by immunoblot. We found that expression of NLRP7 was sufficient to cause high molecular weight NLRP7 complexes as large as 670 kDa. However, NLRP7^{WA} exhibited significantly reduced ability to assemble into high molecular weight complexes and was found primarily in fractions corresponding to its monomeric form of 110 kDa (Fig. 2D). Collectively, these data demonstrate that NLRP7 oligomerization is likely nucleotide dependent, as mutation in the Walker A motif substantially reduced its ability to form the high molecular weight complexes characteristic of NLRP7.

3.3. The NLRP7 NBD has ATP-binding and hydrolysis activities

Since the Walker A motif was required for self-association, we next tested whether NLRP7 is capable of nucleotide binding through its NBD. We expressed myc-tagged NLRP7^{NBD} in HEK293 cells and performed an ATP-binding assay, by purifying ATP binding proteins from total cell lysates with immobilized ATP-coated agarose beads. ATP agarose, but not control agarose pulled down NLRP7^{NBD}. This interaction was specific, as free ATP in the binding buffer competed for NLRP7^{NBD} binding in a dose-dependent manner (Fig. 3A, upper panel). Contrary to the NLRP7^{NBD}, the NLRP7$^{NBD(WA)}$ failed to bind ATP (Fig. 3A, bottom panel). These data suggest that the NBD of NLRP7 binds ATP and that the Walker A motif is necessary for ATP binding. Since ATP binding is a prerequisite for its hydrolysis, we next tested whether NLRP7^{NBD} was able to hydrolyze the bound ATP. We employed an ATPase detection assay using a luminescent readout to quantify ATP hydrolysis. We purified GST-NLRP7^{NBD}, GST-NLRP7$^{NBD(WA)}$ and GST control from bacteria (Fig. 3B) and subjected these proteins to the *in vitro* ATPase assay. GST-NLRP7^{NBD}, but not GST control revealed a dose dependent increase in ATP hydrolysis (Fig. 3C), indicating that the NLRP7^{NBD} contains ATPase activity. Importantly, the NLRP7$^{NBD(WA)}$ protein displayed significantly reduced ATPase activity, when compared to NLRP7^{NBD} (Fig. 3D), demonstrating that an intact Walker A motif was required for both ATP binding and hydrolysis.

3.4. The NLRP7 Walker A motif is required for inflammasome activation

Our results so far collectively demonstrate that NLRP7 oligomerizes through homomeric self-association of its NBD in an ATP-dependent manner, suggesting that this process is involved in NLRP7 inflammasome assembly. To directly determine the role of ATP binding in NLRP7 inflammasome activity, we reconstituted the NLRP7 inflammasome in HEK293 cells, which are deficient in this inflammasome, but can be used to transiently restore NLRP7 activity (Khare et al., 2012). As we showed earlier, reconstitution of the NLRP7 inflammasome by co-transfecting the core inflammasome components ASC, pro-caspase-1, pro-IL-1β and NLRP7 results in the release of mature IL-1β into the culture supernatant, as

detected by ELISA, which is comparable to reconstituted NLRP3 inflammasomes (Khare et al., 2012) (Fig. 4A). In contrast, reconstituting the NLRP7 inflammasome with NLRP7^{WA} failed to promote IL-1β release (Fig. 4A). Transfection of low amounts of NLRP7 allows the subsequent inflammasome activation with FSL-1, a microbial acLP agonist for NLRP7 (Khare et al., 2012). While reconstituted NLRP7 inflammasomes responded to FSL-1 with increased IL-1β release, inflammasomes reconstituted with NLRP7^{WA} were unable to respond to FSL-1 (Fig. 4B). Total cell lysates were analyzed for equal expression of NLRP3, NLRP7 and NLRP7^{WA} by immunoblot (Fig. 4C). Sine caspase-1 is required for inflammasome-mediated cytokine release, we also directly determined caspase-1 activation in this inflammasome reconstitution assay by immunoblot. Consistent with the reduced IL-1β release of NLRP7^{WA} reconstituted inflammasomes, also caspase-1 activation, which was determined by the conversion of pro-caspase-1 p45 into caspase-1 p10, which is a consequence of caspase-1 activation, was strongly reduced in NLRP7^{WA} reconstituted inflammasomes compared to NLRP7 reconstituted inflammasomes (Fig. 4D). We further validated this finding by re-probing the immunoblot with an antibody specific for active caspase-1 p20, which confirmed that NLRP7^{WA} reconstituted inflammasomes are defect in activating caspase-1 (Fig. 4D). Collectively, these experiments indicate that the Walker A motif is essential for NLRP7 inflammasome activity, which further suggests a functional role for ATP binding and hydrolysis in NLRP7 signaling.

3.5. Monocytes expressing Walker A deficient NLRP7 are impaired in acylated lipopeptide-induced inflammasome activation

To directly demonstrate that ATP binding and hydrolysis is required for NLRP7 inflammasome activation we utilized the human THP-1 cell line, which is routinely used for inflammasome studies. We generated stable THP-1 cells expressing either myc-tagged NLRP7 or NLRP7^{WA} or a vector control (Fig. 5A). We then treated these THP-1 cells with agonists that activate NLRP7, including FSL-1, Pam_3CSK_4 or heat killed mycoplasma *Acholeplasma laidlawii* (HKAL) (Khare et al., 2012) and determined secretion of IL-1β as a readout for inflammasome activation. THP-1^{NLRP7} cells secreted elevated levels of IL-1β in response to NLRP7 agonists, when compared to control THP-1^{Ctrl} cells, as expected due to the increased expression of NLRP7 (Fig. 5B). In contrast, THP-1$^{NLRP7(WA)}$ cells secreted significantly diminished IL-1β into culture supernatants (Fig. 5B), indicating that a NBD with intact Walker A motif is required for NLRP7 inflammasome activation, which validates our findings from the inflammasome reconstitution system. The fact that THP-1$^{NLRP7(WA)}$ cells secreted less IL-1β than THP-1^{Ctrl} cells in response to HKAL suggests that under these conditions NLRP7^{WA} may even generate a dominant negative phenotype. To directly determine caspase-1 activation, we infected THP-1^{Ctrl}, THP-1^{NLRP7} and THP-1$^{NLRP7(WA)}$ cells with *S. aureus* for 0, 15 and 60 min and immunoprobed total cell lysates and conditioned culture supernatants for pro-caspase-1. Pro-caspase-1 expression was comparable in all three cell lines, and *S. aureus* infection resulted in the appearance of active caspase-1 in total cell lysates and in culture supernatants of THP-1^{Ctrl} cells by 60 min (Fig. 5C). However, THP-1^{NLRP7} cells displayed increased caspase-1 activity, since active caspase-1 was already detected after 15 min in total cell lysates and by 60 min most of the active caspase-1 accumulated in culture supernatants (Fig. 5C). In contrast, active caspase-1 was not detectable in total cell lysates in THP-1$^{NLRP7(WA)}$ cells and was consequently also

reduced in culture supernatants (Fig. 5C). Caspase-1 activation also causes pyroptosis, a lytic form of cell death, which consequently causes membrane permeability for DAMPs and other large molecules. Therefore Propidium iodide (PI) (670 Da), which is usually unable to pass through membranes, can be taken up by cells undergoing pyroptosis and emits fluorescence light upon intercalation into double stranded DNA (Fink and Cookson, 2006). Hence to quantify pyroptosis we monitored uptake and DNA binding of PI by kinetic fluorescence assay. While THP-1^{NLRP7} cells displayed PI DNA binding after 10–15 min of *S. aureus* infection, consistent with the detection of active caspase-1 (Fig. 5D), THP-1$^{NLRP7(WA)}$ cells showed significantly reduced PI uptake and DNA binding (Fig. 5D), in agreement with strongly reduced active caspase-1. Since caspase-1 activation is a direct consequence of NLRP7 activation in response to acLPs and *S. aureus* infection, our results indicate that intact nucleotide binding is required for inflammasome activation.

4. Discussion

Caspase-1 is activated by induced proximity, which occurs within inflammasomes and requires oligomeric inflammasome complexes. ASC polymerization promotes the required caspase-1 density and prion-like self propagating ASC polymerization itself is nucleated by upstream PRRs, as demonstrated for NLRP3 and AIM2 (Cai et al., 2014; Lu et al., 2014; Man et al., 2014; Franklin et al., 2014). ASC nucleation is vastly enhanced by oligomerized PRRs, thus supporting the necessity for PRR self interaction (Lu et al., 2014). We previously identified the role of NLRP7 as an inflammasome-activating PRR in human macrophages (Khare et al., 2012). NLRP7 inflammasome activation occurs in response to *S. aureus* and *L. monocytogenes* infection by sensing acLP PAMPs. In response to bacterial infection, NLRP7 inflammasome activity coincided with its ability to assemble high molecular weight complexes containing also the inflammasome adaptor ASC and caspase-1. However, the molecular mechanism responsible for NLRP7 inflammasome assembly has not yet been elucidated. Here we demonstrate that NLRP7 binds and hydrolyzes ATP through its predicted NBD and that this activity is necessary for NLRP7 oligomerization and inflammasome activation, reminiscent of NLRP3 (Duncan et al., 2007). During the preparation of our manuscript, El-Maarri and colleagues demonstrated that the NLRP7^{NAD} is required for NLPR7 dimerization (Singer et al., 2014). We extend this finding to demonstrate that ATP binding and hydrolysis is essential for oligomerization and inflammasome activation in response to acLPs and *S. aureus*, thus demonstrating a functional consequence of ATP binding.

The current model of NLR activation was largely deducted from our understanding of the STAND family ATPase APAF-1 and its nucleotide-dependent activation model in apoptosome formation, but has recently also been demonstrated for NLRC4, based on its crystal structure (Hu et al., 2013). Based on our results, NLRP7 joins several other NLRPs with experimentally demonstrated nucleotide binding and hydrolysis activities, including NLRP1, NLRP3 and NLRP12, which all commonly form large protein platforms for signal transduction (Faustin et al., 2007; Ye et al., 2008; Duncan et al., 2007). While the NLRP7$^{NBD(WA)}$, which we show to be deficient in ATP binding and hydrolysis, showed reduced self-association with NLRP7^{NBD}, the NLRP7$^{NBD(WA)}$ completely failed to self interact with itself.

There is significant interest in leveraging inflammasome-assembling NLRs as molecular targets for therapeutics, as several have been linked to inflammatory disease. Although current treatments for inflammasome-linked diseases (*i.e.*, Cyropyrinopathies) target upstream or downstream effectors such as secondary messengers, cytokines and cytokine receptors, the NLR may serve as a potential target upstream of caspase-1 activation. In fact several anti-inflammatory compounds target NLRP3, including its ATPase activity (Juliana et al., 2010; Gong et al., 2010; Lamkanfi et al., 2009). Consequently, the NBD, in particular the Walker A motif, has been proposed as a target for the structure guided design of specific ATPase inhibitors to allow selective targeting of individual NLRs, including NLRP7 (MacDonald et al., 2013).

Hereditary mutations in *NLRP7* are associated with recurrent hydatidiform moles (HM), which increase risk for molar pregnancy and choriocarcinoma in women (Messaed et al., 2011a,b; Murdoch et al., 2006; Nguyen and Slim, 2014). However, the relationship between NLRP7 inflammasome function and the development of HM is currently not understood, however altered cytokine secretion has been proposed (Messaed et al., 2011a,b). We previously reported that several HM-linked mutations yield gain-of-function phenotypes in a reconstituted inflammasome system (Khare et al., 2012). In agreement, a recent study indicated that certain HM-linked mutations within the NACHT increase NLRP7 oligomerization by destabilizing the closed NACHT conformation (Singer et al., 2014). However, HM-linked mutations have not been identified within the Walker A motif (Touitou et al., 2004), which according to our results would yield in a loss-of-function phenotype. Since we show that an intact Walker A motif is required for oligomerization, ATP binding and hydrolysis by NLRP7 may contribute to HM, and therapies targeting this process may potentially be effective in HM patients. Therefore our study identifying ATP binding and hydrolysis as an essential step for NLRP7 inflammasome activation not only establishes the basis for such a strategy, but also provides novel insights into the mechanism of NLRP7 inflammasome activation.

Supplementary Material

Refer to Web version on PubMed Central for supplementary material.

Acknowledgments

This work was supported by the National Institutes of Health (GM071723, AI099009 and AR064349 to C.S., AR057532 and AR066739 to A.D.), the Skin Disease Research Center (AR057216) and the American Heart Association (12GRNT12080035) to C.S., S.K. was an Arthritis Foundation fellow (AF161715) and L.H.C. was supported by the Vietnam Education Foundation and the American Heart Association (15PRE25700116). Plasmids pMD2.G and psPAX2 were kindly provided by Didier Trono (École Polytechnique Fédérale de Lausanne).

Abbreviations

acLP	acetylated lipopeptides
ASC	apoptosis-associated speck-like protein containing a CARD
ATPase	adenosine triphosphatases

CARD	caspase recruitment domain
DAMP	damage associated molecular pattern
FLICA	fluorescent labeled inhibitor of caspase-1 assay
HEK293	human embryonic kidney 293 cells
HKAL	heat killed *Acholeplasma laidlawii*
HM	hydatidiform moles
IL-1β	interleukin-1β
LRR	leucine rich repeat
NACHT	NAIP, CIITAHET-E and TP1
NAD	NACHT associated domain
NBD	nucleotide binding domain
NLR	nucleotide binding oligomerization domain (NOD)-like receptor
NLRP7	NLR containing a PYD domain 7
PAMP	pathogen associated molecular pattern
PI	Propidium iodide
PRR	pattern recognition receptor
PYD	PYRIN domain
S. aureus	*Staphylococcus aureus*
WA	Walker A

References

Albrecht M, Domingues FS, Schreiber S, Lengauer T. Structural localization of disease-associated sequence variations in the NACHT and LRR domains of PYPAF1 and NOD2. FEBS Lett. 2003; 554:520–528. [PubMed: 14623123]

Baroja-Mazo A, Martín-Sánchez F, Gomez AI, Martínez CM, Amores-Iniesta J, Compan V, Barberà-Cremades M, Yagüe J, Ruiz-Ortiz E, et al. The NLRP3 inflammasome is released as a particulate danger signal that amplifies the inflammatory response. Nat Immunol. 2014; 15:738–748. [PubMed: 24952504]

Bryan NB, Dorfleutner A, Kramer SJ, Yun C, Rojanasakul Y, Stehlik C. Differential splicing of the apoptosis-associated speck like protein containing a caspase recruitment domain (ASC) regulates inflammasomes. J Inflamm (Lond). 2010; 7:23. [PubMed: 20482797]

Cai X, Chen J, Xu H, Liu S, Jiang QX, Halfmann R, Chen ZJ. Prion-like polymerization underlies signal transduction in antiviral immune defense and inflammasome activation. Cell. 2014; 156:1207–1222. [PubMed: 24630723]

Chu LH, Gangopadhyay A, Dorfleutner A, Stehlik C. An updated view on the structure and function of PYRIN domains. Apoptosis. 2015; 20:157–173. [PubMed: 25451010]

Danot O, Marquenet E, Vidal-Ingigliardi D, Richet E. Wheel of life wheel of death: a mechanistic insight into signaling by STAND proteins. Structure. 2009; 17:172–182. [PubMed: 19217388]

Dorfleutner A, Bryan NB, Talbott SJ, Funya KN, Rellick SL, Reed JC, Shi X, Rojanasakul Y, Flynn DC, Stehlik C. Cellular pyrin domain-only protein 2 is a candidate regulator of inflammasome activation. Infect Immun. 2007a; 75:1484–1492. [PubMed: 17178784]

Dorfleutner A, Talbott SJ, Bryan NB, Funya KN, Reed JC, Shi X, Flynn DC, Rojanasakul Y, Stehlik C. A Shope Fibroma virus PYRIN-only protein modulates the host immune response. Virus Genes. 2007b; 35:685–694. [PubMed: 17676277]

Duncan JA, Bergstralh DT, Wang Y, Willingham SB, Ye Z, Zimmermann AG, Ting JP. Cryopyrin/NALP3 binds ATP/dATP, is an ATPase, and requires ATP binding to mediate inflammatory signaling. Proc Natl Acad Sci U S A. 2007; 104:8041–8046. [PubMed: 17483456]

Eibl C, Grigoriu S, Hessenberger M, Wenger J, Puehringer S, Pinheiro AS, Wagner RN, Proell M, Reed JC, et al. Structural and functional analysis of the NLRP4 pyrin domain. Biochemistry. 2012; 51:7330–7341. [PubMed: 22928810]

Fantuzzi G, Reed DA, Dinarello CA. IL-12-induced IFN-gamma is dependent on caspase-1 processing of the IL-18 precursor. J Clin Investig. 1999; 104:761–767. [PubMed: 10491411]

Faustin B, Lartigue L, Bruey JM, Luciano F, Sergienko E, Bailly-Maitre B, Volkmann N, Hanein D, Rouiller I, Reed JC. Reconstituted NALP1 inflammasome reveals two-step mechanism of caspase-1 activation. Mol Cell. 2007; 25:713–724. [PubMed: 17349957]

Fink SL, Cookson BT. Caspase-1-dependent pore formation during pyroptosis leads to osmotic lysis of infected host macrophages. Cell Microbiol. 2006; 8:1812–1825. [PubMed: 16824040]

Franklin BS, Bossaller L, De Nardo D, Ratter JM, Stutz A, Engels G, Brenker C, Nordhoff M, Mirandola SR, et al. The adaptor ASC has extracellular and 'prionoid' activities that propagate inflammation. Nat Immunol. 2014; 15:727–737. [PubMed: 24952505]

Ghayur T, Banerjee S, Hugunin M, Butler D, Herzog L, Carter A, Quintal L, Sekut L, Talanian R, et al. Caspase-1 processes IFN-gamma-inducing factor and regulates LPS-induced IFN-gamma production. Nature. 1997; 386:619–623. [PubMed: 9121587]

Gong YN, Wang X, Wang J, Yang Z, Li S, Yang J, Liu L, Lei X, Shao F. Chemical probing reveals insights into the signaling mechanism of inflammasome activation. Cell Res. 2010; 20:1289–1305. [PubMed: 20856264]

Groß O, Yazdi A, Thomas C, Masin M, Heinz L, Guarda G, Quadroni M, Drexler S, Tschopp J. Inflammasome activators induce interleukin-1α secretion via distinct pathways with differential requirement for the protease function of caspase-1. Immunity. 2012; 36:388–400. [PubMed: 22444631]

Harton JA, Cressman DE, Chin KC, Der CJY, Ting JP. GTP binding by class II transactivator: role in nuclear import. Science. 1999; 285:1402. [PubMed: 10464099]

Hu Z, Yan C, Liu P, Huang Z, Ma R, Zhang C, Wang R, Zhang Y, Martinon F, et al. Crystal structure of NLRC4 reveals its autoinhibition mechanism. Science. 2013; 341:172–175. [PubMed: 23765277]

Iyer LM, Leipe DD, Koonin EV, Aravind L. Evolutionary history and higher order classification of AAA+ ATPases. J Struct Biol. 2004; 146:11–31. [PubMed: 15037234]

Juliana C, Fernandes-Alnemri T, Wu J, Datta P, Solorzano L, Yu JW, Meng R, Quong AA, Latz E, et al. Anti-inflammatory compounds parthenolide and Bay 11-7082 are direct inhibitors of the inflammasome. J Biol Chem. 2010; 285:9792–9802. [PubMed: 20093358]

Khare S, Luc N, Dorfleutner A, Stehlik C. Inflammasomes and their activation. Crit Rev Immunol. 2010; 30:463–487. [PubMed: 21083527]

Khare S, Dorfleutner A, Bryan NB, Yun C, Radian AD, de Almeida L, Rojanasakul Y, Stehlik C. An NLRP7-containing inflammasome mediates recognition of microbial lipopeptides in human macrophages. Immunity. 2012; 36:464–476. [PubMed: 22361007]

Kinoshita T, Wang Y, Hasegawa M, Imamura R, Suda T. PYPAF3, a PYRIN-containing APAF-1-like protein, is a feedback regulator of caspase-1-dependent interleukin-1beta secretion. J Biol Chem. 2005; 280:21720–21725. [PubMed: 15817483]

Koonin EV, Aravind L. The NACHT family-a new group of predicted NTPases implicated in apoptosis and MHC transcription activation. Trends Biol Sci. 2000; 25:223–224.

Kostura MJ, Tocci MJ, Limjuco G, Chin J, Cameron P, Hillman AG, Chartrain NA, Schmidt JA. Identification of a monocyte specific pre-interleukin 1 beta convertase activity. Proc Natl Acad Sci. 1989; 86:5227–5231. [PubMed: 2787508]

Kuida K, Lippke JA, Ku G, Harding MW, Livingston DJ, Su MS, Flavell RA. Altered cytokine export and apoptosis in mice deficient in interleukin-1 beta converting enzyme. Science. 1995; 267:2000–2003. [PubMed: 7535475]

Lamkanfi M, Mueller JL, Vitari AC, Misaghi S, Fedorova A, Deshayes K, Lee WP, Hoffman HM, Dixit VM. Glyburide inhibits the cryopyrin/Nalp3 inflammasome. J Cell Biol. 2009; 187:61–70. [PubMed: 19805629]

Lamkanfi M, Sarkar A, Vande Walle L, Vitari AC, Amer AO, Wewers MD, Tracey KJ, Kanneganti TD, Dixit VM. Inflammasome-dependent release of the alarmin HMGB1 in endotoxemia. J Immunol. 2010; 185:4385–4392. [PubMed: 20802146]

Leipe DD, Koonin EV, Aravind L. STAND, a class of P-loop NTPases including animal and plant regulators of programmed cell death: multiple, complex domain architectures, unusual phyletic patterns, and evolution by horizontal gene transfer. J Mol Biol. 2004; 343:1–28. [PubMed: 15381417]

Li P, Allen H, Banerjee S, Franklin S, Herzog L, Johnston C, McDowell J, Paskind M, Rodman L, et al. Mice deficient in IL-1b-converting enzyme are defective in production of mature IL-1b and resistant to endotoxic shock. Cell. 1995; 80:401–411. [PubMed: 7859282]

Lu A, Magupalli VG, Ruan J, Yin Q, Atianand MK, Vos MR, Schröder GF, Fitzgerald KA, Wu H, Egelman EH. Unified polymerization mechanism for the assembly of ASC-dependent inflammasomes. Cell. 2014; 156:1193–1206. [PubMed: 24630722]

Lu C, Wang A, Wang L, Dorsch M, Ocain TD, Xu Y. Nucleotide binding to CARD12 and its role in CARD12-mediated caspase-1 activation. Biochem Biophys Res Commun. 2005; 331:1114–1119. [PubMed: 15882992]

MacDonald JA, Wijekoon CP, Liao KC, Muruve DA. Biochemical and structural aspects of the ATP-binding domain in inflammasome-forming human NLRP proteins. IUBMB Life. 2013; 65:851–862. [PubMed: 24078393]

Man SM, Hopkins LJ, Nugent E, Cox S, Glück IM, Tourlomousis P, Wright JA, Cicuta P, Monie TP, Bryant CE. Inflammasome activation causes dual recruitment of NLRC4 and NLRP3 to the same macromolecular complex. Proc Natl Acad Sci U S A. 2014; 111:7403–7408. [PubMed: 24803432]

Martinon F, Burns K, Tschopp J. The inflammasome: a molecular platform triggering activation of inflammatory caspases and processing of proIL-beta. Mol Cell. 2002; 10:417–426. [PubMed: 12191486]

Meissner TB, Li A, Liu YJ, Gagnon E, Kobayashi KS. The nucleotide-binding domain of NLRC5 is critical for nuclear import and transactivation activity. Biochem Biophys Res Commun. 2012; 418:786–791. [PubMed: 22310711]

Messaed C, Akoury E, Djuric U, Zeng J, Saleh M, Gilbert L, Seoud M, Qureshi S, Slim R. NLRP7, a NOD-like receptor protein, is required for normal cytokine secretion and co-localizes with the Golgi and the microtubule organizing center. J Biol Chem. 2011a; 286:43313–43323. [PubMed: 22025618]

Messaed C, Chebaro W, Di Roberto RB, Rittore C, Cheung A, Arseneau J, Schneider A, Chen MF, Bernishke K, et al. NLRP7 in the spectrum of reproductive wastage: rare non-synonymous variants confer genetic susceptibility to recurrent reproductive wastage. J Med Genet. 2011b; 48:540–548. [PubMed: 21659348]

Murdoch S, Djuric U, Mazhar B, Seoud M, Khan R, Kuick R, Bagga R, Kircheisen R, Ao A, et al. Mutations in NALP7 cause recurrent hydatidiform moles and reproductive wastage in humans. Nat Genet. 2006; 38:300–302. [PubMed: 16462743]

Nguyen NMP, Slim R. Genetics and epigenetics of recurrent hydatidiform moles: basic science and genetic counselling. Curr Obstet Gynecol Rep. 2014; 3:55–64. [PubMed: 24533231]

Proell M, Riedl SJ, Fritz JH, Rojas AM, Schwarzenbacher R. The Nod-like receptor (NLR) family: a tale of similarities and differences. PLoS ONE. 2008; 3:e2119. [PubMed: 18446235]

Radian AD, de Almeida L, Dorfleutner A, Stehlik C. NLRP7 and related inflammasome activating pattern recognition receptors and their function in host defense and disease. Microbes Infect. 2013; 15:630–639. [PubMed: 23618810]

Ratsimandresey RA, Dorfleutner A, Stehlik C. An update on PYRIN domain-containing pattern recognition receptors: from immunity to pathology. Front Immunol. 2013; 4:440. [PubMed: 24367371]

Reubold TF, Wohlgemuth S, Eschenburg S. Crystal structure of full-length Apaf-1: how the death signal is relayed in the mitochondrial pathway of apoptosis. Structure. 2011; 19:1074–1083. [PubMed: 21827944]

Riedl SJ, Li W, Chao Y, Schwarzenbacher R, Shi Y. Structure of the apoptotic protease-activating factor 1 bound to ADP. Nature. 2005; 434:926–933. [PubMed: 15829969]

Schroder K, Tschopp J. The inflammasomes. Cell. 2010; 140:821–832. [PubMed: 20303873]

Singer H, Biswas A, Zimmer N, Messaed C, Oldenburg J, Slim R, El-Maarri O. NLRP7 inter-domain interactions: the NACHT-associated domain (NAD) is the physical mediator for oligomeric assembly. Mol Hum Reprod. 2014

Srinivasula SM, Poyet JL, Razmara M, Datta P, Zhang Z, Alnemri ES. The PYRIN-CARD protein ASC is an activating adaptor for caspase-1. J Biol Chem. 2002; 277:21119–21122. [PubMed: 11967258]

Stehlik C, Lee SH, Dorfleutner A, Stassinopoulos A, Sagara J, Reed JC. Apoptosis-associated speck-like protein containing a caspase recruitment domain is a regulator of procaspase-1 activation. J Immunol. 2003a; 171:6154–6163. [PubMed: 14634131]

Stehlik C, Krajewska M, Welsh K, Krajewski S, Godzik A, Reed JC. The PAAD/PYRIN-only protein POP1/ASC2 is a modulator of ASC-mediated NF-kB and pro-caspase-1 regulation. Biochem J. 2003b; 373:101–113. [PubMed: 12656673]

Thornberry NA, Bull HG, Calaycay JR, Chapman KT, Howard AD, Kostura MJ, Miller DK, Molineaux SM, Weidner JR, et al. A novel heterodimeric cysteine protease is required for interleukin-1 beta processing in monocytes. Nature. 1992; 356:768–774. [PubMed: 1574116]

Touitou I, Lesage S, McDermott M, Cuisset L, Hoffman H, Dode C, Shoham N, Aganna E, Hugot JP, et al. Infevers: an evolving mutation database for auto-inflammatory syndromes. Hum Mutat. 2004; 24:194–198. [PubMed: 15300846]

Traut TW. The functions and consensus motifs of nine types of peptide segments that form different types of nucleotide-binding sites. Eur J Biochem. 1994; 222:9–19. [PubMed: 8200357]

Willingham SB, Allen IC, Bergstralh DT, Brickey WJ, Huang MTH, Taxman DJ, Duncan JA, Ting JPY. NLRP3 (NALP3, cryopyrin) facilitates in vivo caspase-1 activation, necrosis, and HMGB1 release via inflammasome-dependent and -independent pathways. J Immunol. 2009; 183:2008–2015. [PubMed: 19587006]

Ye Z, Lich JD, Moore CB, Duncan JA, Williams KL, Ting JP. ATP binding by monarch-1/NLRP12 is critical for its inhibitory function. Mol Cell Biol. 2008; 28:1841–1850. [PubMed: 18160710]

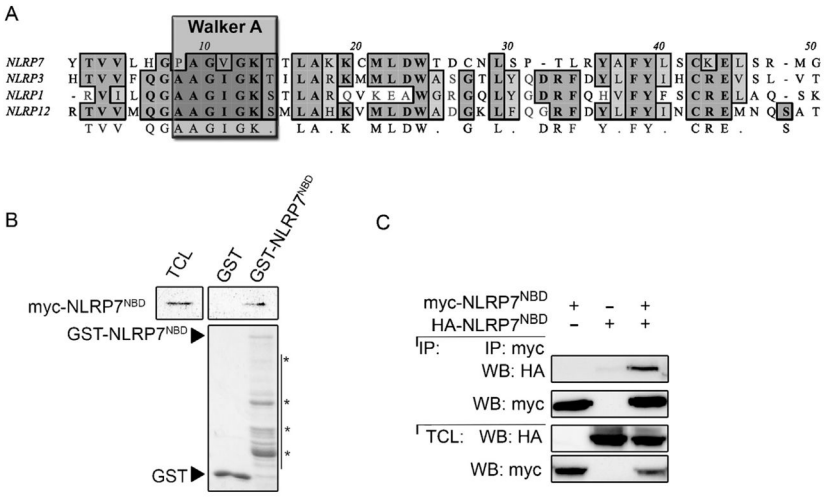

Fig. 1.

NLRP7 contains a predicted nucleotide-binding domain (NBD), which is sufficient for dimerization. (A) CLUSTAL-W sequence alignment of the NLRP7^{NBD} Walker A motif with the NBD of NLRP members with experimentally confirmed nucleotide binding and ATPase activity. The Walker A motif, containing the phosphate-binding loop, is outlined. (B) *In vitro* GST pull-down of immobilized GST-NLRP7^{NBD} using total cell lysates (TCL) from HEK293 cells transiently transfected with myc-NLRP7^{NBD} and immobilized GST as a negative control. Bound NLRP7^{NBD} was detected by immunoblot with anti-myc antibodies. Blots were stripped and re-probed with anti-GST antibodies. 5% TCL were loaded as input. (C) HEK293 cells were transiently co-transfected with HA- and myc-tagged NLRP7^{NBD} proteins and TCL subjected to co-immunopreciptation (IP) using immobilized anti-myc antibodies and bound proteins were detected by immunoblot with anti-HA antibodies. Blots were stripped and re-probed with anti-myc antibodies. 5% TCL were loaded as input.

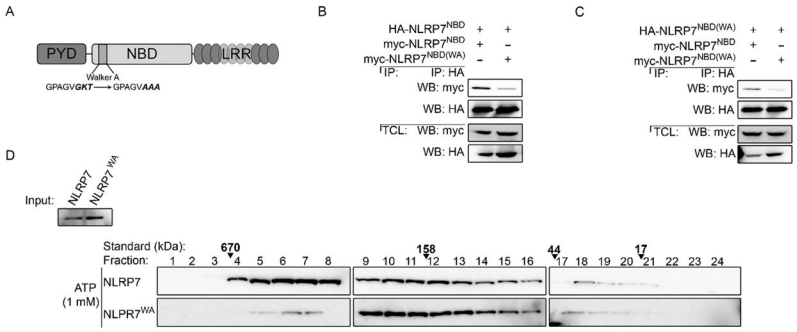

Fig. 2.

The Walker A motif in the NBD is required for NLRP7 oligomerization. (A) Domain architecture of NLRP7 depicting the Walker A mutation GKT to AAA. PYD: Pyrin domain, LRR: leucine-rich repeats. (B, C) HEK293 cells were transiently co-transfected with HA- and myc-tagged NLPR7^{NBD} and/or NLRP7$^{NBD(WA)}$ as indicated. Total cell lysates (TCL) were subjected to co-immunopreciptation (IP) using immobilized anti-HA antibodies and bound proteins were detected by immunoblot with anti-myc antibodies. Blots were stripped and re-probed with anti-HA antibodies. 2% TCL were loaded as input. (D) HEK293 cells were transfected with myc-tagged NLRP7 or NLRP7^{WA}, and TCL supplemented with 1 mM ATP were subjected to size exclusion chromatography (SEC). Individual fractions were TCA precipitated and analyzed by immunoblot using anti-myc antibodies. Fraction numbers from largest to smallest are indicated on top, alongside a molecular weight standard, which was separated under identical conditions. 2% TCL were loaded as input.

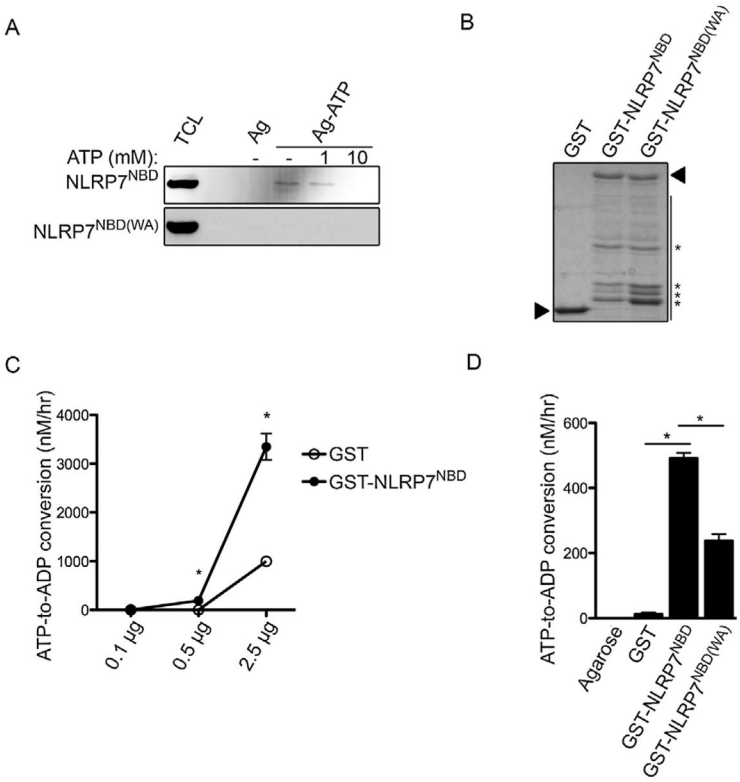

Fig. 3.

NLRP7 binds and hydrolyzes ATP through its NBD. (A) *In vitro* pull-down of ATP-conjugated agarose beads (Ag-ATP) and control agarose beads (Ag) using lysates from HEK293 cells transiently transfected with either myc-tagged NLRP7^{NBD} or NLRP7$^{NBD(WA)}$, as indicated. Binding buffers were supplemented with free ATP (0, 1 and 10 mM), as indicated to specifically compete for binding of Ag-ATP to the NBD. (B) Recombinant GST-NLRP7^{NBD} and NLRP7$^{NBD(WA)}$ proteins were expressed and affinity purified from BL21 *Escherichia coli*. 1 µg protein was separated by SDS-PAGE and detected by Coomassie stain. Triangles mark the full length proteins and asterisks mark several degradation products of the NBD. (C) *In vitro* ATPase assay showing dose-dependent *in vitro* ATP hydrolysis by recombinant NLRP7^{NBD} using GST as a control with 0, 0.1, 0.5 and 2.5 µg protein as indicated. (D) Endpoint quantification of NLRP7^{NBD} and NLRP7$^{NBD(WA)}$ ATP hydrolysis activity. Results are presented as ATP to ADP conversion nM/hr ($n = 3 \pm$ SEM). *$P < 0.05$.

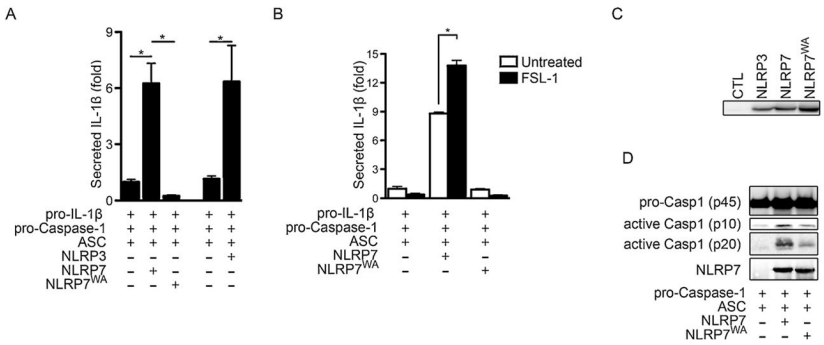

Fig. 4.

NLRP7WA is deficient in IL-1β release in a reconstituted inflammasome assay. (A, B) Inflammasomes were reconstituted by transient transfection of HEK293 cells with the inflammasome core components ASC, pro-Caspase-1, pro-IL-1β and either NLRP7, NLRP7^{WA}, NLRP3 or empty vector control, as indicated. Secreted IL-1β was determined from conditioned culture supernatants by ELISA 36 h post transfection. (B) Cells were transfected as in (A), followed by a second transfection after 24 h with transfection reagent alone (untreated) or FSL-1 (0.5 μg). IL-1β was determined by ELISA 12 h after the second transfection. Results are presented as fold increase compared to cells transfected with ASC, pro-Caspase-1, pro-IL-1β, and empty vector control (EV control) ($n = 3 \pm$ SEM). *$P < 0.05$. (C) Immunoblot demonstrating expression of myc-NLRP3 and NLRP7 in the reconstitution assay. (D) Immunoblot of cell lysates from the inflammasome reconstitution assay analyzed for pro-caspase-1, cleaved caspase-1 p10, active caspase-1 p20 and NLRP7.

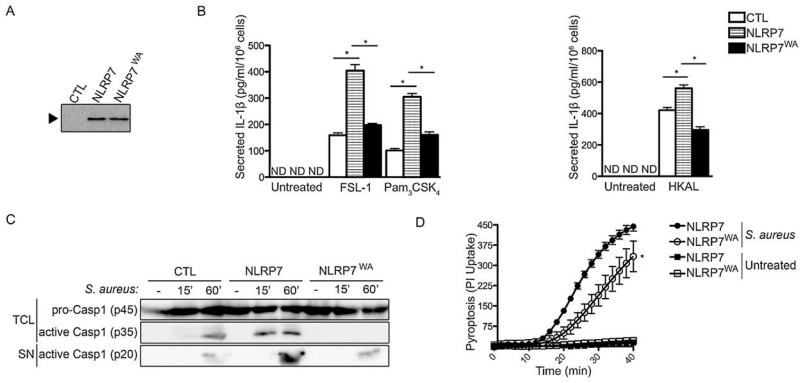

Fig. 5.

THP-1 cells expressing NLRP7^{WA} are defect in acylated lipopeptide- and *S. aureus*-induced inflammasome activation. (A) Anti-myc immunoprecipitates from cell lysates of stable THP-1 cells expressing myc control (CTL), myc-NLRP7 or myc-NLRP7^{WA} were analyzed by immunoblot using anti-myc antibodies to confirm comparable expression levels. (B) Stable THP-1 cells were either left untreated, treated with FSL-1 (100 ng/ml), Pam_3CSK_4 (100 ng/ml) or HKAL (1×10^5 CFU) for 4 h and culture supernatants were analyzed for secreted IL-1β by ELISA ($n = 3 \pm$ s.e.m.). *$P < 0.05$. (C) Stable THP-1 cells were infected with *S. aureus* for 0, 15 or 60 min, and TCA precipitated conditioned culture supernatants (SN) and total cell lysates (TCL) were analyzed by immunoblot for pro-Caspase-1 or active Caspase-1 p35 in TCL and p20 in SN. (D) Stable THP-1 cells were infected with *S. aureus* in white 96-well plates and propidium iodide (PI) uptake was quantified by kinetic fluorescence assay upon DNA binding ($n = 3 \pm$ s.e.m.). *$P < 0.05$.